Comparison of ERA5 and ERA-Interim near surface air temperature and precipitation over Arctic sea ice: Effects on sea ice thermodynamics and evolution

Caixin Wang[1, 2], Robert M. Graham[2], Keguang Wang[1], Sebastian Gerland[2], Mats A. Granskog[2]

5 [1]Norwegian Meteorological Institute, Tromsø, 9293, Norway

[2]Norwegian Polar Institute, Fram Centre, Tromsø, 9296, P.O.Box 6606 Langnes, Norway

Correspondence to: Caixin Wang (caixin.wang@npolar.no)

Abstract. Rapid changes are occurring in the Arctic, including a reduction in sea ice thickness and coverage and a shift towards younger and thinner sea ice. Snow and sea ice models are often used to study these ongoing changes in the Arctic, and are

10 typically forced by atmospheric reanalyses in absence of observations. ERA5 is a new global reanalysis that will replace the widely used ERA-Interim (ERA-I). In this study, we compare the 2 m air temperature (T2M) and precipitation between ERA-I and ERA5, and evaluate these products using buoy observations from Arctic sea ice. We further assess how biases in reanalyses influence the snow and sea ice evolution in the Arctic, when used to force a thermodynamic sea ice model. We find that both reanalyses have a warm bias over Arctic sea ice in relation to the buoy observations. The warm bias is smaller in the warm

15 season, and larger in the cold season, especially when the T2M is lower than -25°C. Interestingly, the warm bias in the new ERA5 is on average 2.1 °C (daily mean) larger than ERA-I during the cold season. While ERA-I is drier than most modern reanalyses in the Arctic, the total precipitation along the buoy trajectories is often lower in ERA5 than in ERA-I. Nonetheless, the snowfall products are broadly similar for both ERA-I and ERA5. ERA-I had substantial anomalous Arctic rainfall, which is greatly reduced in ERA5. Simulations with a freezing degree days (FDD) model and a 1D thermodynamic sea ice model

20 demonstrate that the warm bias in ERA5 acts to reduce thermodynamic ice growth. However, the lower precipitation in ERA5 results in a thinner snow pack that allows more heat loss to the atmosphere. Thus, the larger warm bias and lower precipitation in ERA5, compared with ERA-I, compensate in terms of the effect on winter ice growth. Ultimately, we find slightly thicker ice at the end of growth season when using ERA5 forcing, compared with ERA-I. Thus differences in the precipitation fields of the two reanalyses have a larger influence on the sea ice evolution than the T2M.

25 ## 1 Introduction

The Arctic has been undergoing substantial changes in the recent decades. The decline of Arctic sea ice is seen as one of the most prominent indicators of Arctic climate change (Stroeve et al., 2012). The extent and area of the Arctic sea ice has decreased (Comiso et al., 2008), the length of the sea ice melt season is increasing (Markus et al., 2009; Mortin et al., 2014;

Stroeve et al., 2014; Mortin et al., 2016; Stroeve and Notz, 2018), and large areas of thick multi-year ice (MYI) have been replaced by thinner and more dynamic first-year ice (FYI) (Maslanik et al., 2011; Lindsay and Schweiger, 2015; King et al., 2017). The decline of Arctic sea ice has been attributed to various interrelated causes, including a general overall warming trend (Steel et al., 2008; Polyakov et al., 2010). The Arctic is warming more than twice as fast as the global average temperature

5 over the past 50 years (Bekryaev et al., 2010; AMAP, 2017). The fastest warming in the Arctic occurs during the fall and winter season (Graversen et al., 2008; Boisvert and Stroeve, 2015), and is driven in part by an increased number of storms that bring warm winds from the south (Woods and Caballero, 2016; Dahlke and Maturilli, 2017; Graham et al., 2017a, 2017b; Rinke et al., 2017). The additional heat and moisture carried by these storms could contribute to a reduction in the winter ice growth (Woods and Caballero, 2016; Alexeev et al., 2017; Stroeve et al., 2018).

10 Despite the rapid ongoing changes in the Arctic, there are relatively few in-situ atmospheric observations, especially during winter. Due to the lack of in-situ observations, most studies documenting changes in the Arctic rely heavily on atmospheric reanalyses (Screen and Simmonds, 2010; Kapsch et al., 2014; Woods and Caballero, 2016; Sato and Inoue, 2017). However, there are inherent biases and uncertainties within these reanalyses, and large differences can exist among the different products (Tjernstöm and Graversen, 2009; Decker, et al., 2012; Jakobson et al., 2012; Lindsay et al., 2014; Wesslén et al., 2014; Graham

15 et al., 2017b). Atmospheric reanalyses are often used to force snow and sea ice models (Schweiger et al., 2011; Merkouriadi et al., 2017; Stroeve et al., 2018). Thus the choice of reanalysis, and inherent biases within that product, will ultimately influence the simulation of Arctic sea ice mass balance (Cheng et al., 2008; Wang et al., 2015).

The European Centre for Medium-range Weather Forecasts (ECMWF) reanalysis product, ERA-Interim (ERA-I, Dee et al., 2011), has been widely used for studying changes in the Arctic and forcing ocean and sea ice models (e.g., Cheng et al., 2008;

20 Maksimovich and Vihma, 2012; Kapsch et al., 2014; Woods and Caballero, 2016; Graham et al., 2017b). In 2017, the ECMWF released a new reanalysis data ERA5 (Hersbach and Dee, 2016). There are major improvements in ERA5 compared with ERA-I. For example, ERA5 covers a longer period from 1950 (ERA-I from 1979) to present, has higher spatial and temporal resolutions, includes more information on variation in quality over space and time, an improved representation of troposphere, better global balance of precipitation and evaporation, and more consistent sea surface temperature and sea ice coverage

25 (Hersbach and Dee, 2016). Evaluations of the performance of ERA5 have been conducted over the land and revealed a higher performance of ERA5 than ERA-I (Albergel et al., 2018; Urraca et al., 2018), and other commonly used reanalysis, such as, MERRA-2 (the second version of the Modern-Era Retrospective Analysis for Research and Applications) (Olausen, 2018; Urraca et al., 2018). However, the performance of ERA5 over Arctic sea ice is yet to be fully investigated.

In this study, we compare and evaluate the 2 m air temperature (T2M) and precipitation in ERA-I and ERA5 over Arctic

30 sea ice. These are both critical parameters for sea ice simulation (Cheng et al., 2008; Wang et al. 2015). To evaluate the two reanalysis products, we use data from Ice Mass Balance buoys (IMB) (Perovich et al., 2018) and Snow Buoys (Grosfeld et al., 2016; Nicolaus et al., 2017). These buoys typically record position, T2M, mean sea level pressure (MSLP), and snow depth at regular intervals (from hourly to every four hours). We use the T2M and snow depth observations from these buoys to assess

the performance of ERA5 and ERA-I over Arctic sea ice. We further apply a freezing degree day (FDD) model to both reanalyses, and use the reanalyses to force a 1-D thermodynamic sea ice model. The simulations are compared with snow and ice thickness observations from the buoys to evaluate how differences in the T2M and precipitation influence the evolution of sea ice in the model.

2 Materials and Methods

2.1 Buoy data

IMBs autonomously measure thermodynamic changes in sea ice mass balance (Richter-Menge et al., 2006; Polashenski et al., 2011). They are part of a network of drifting buoys over the Arctic Ocean that provide meteorological and oceanographic data for real-time operational requirements and research purposes (Rigor et al., 2000). These instruments typically record GPS position, T2M and mean sea level pressure (MSLP) at hourly intervals, and temperature profiles through the air, snow, ice, and upper-ocean, and distances to snow/ice surface and ice bottom at every four hours. Snow depth and ice thickness can be estimated from the distances knowing the initial thickness of snow and ice when the IMB is deployed (Wang et al., 2013). Similar to IMBs, Snow Buoys also record GPS position, T2M, MSLP, and snow depth at hourly intervals (Grosfeld et al., 2016; Nicolaus et al., 2017). However, Snow Buoys do not measure temperature profiles, and provide no information on ice thickness.

Since 2000, a large number of IMBs have been deployed across the Arctic, in regions such as the Central Arctic, the Beaufort Sea, the Chukchi Sea, the Laptev Sea, the North Pole, Canadian Islands and Svalbard (Perovich et al., 2018) (http://imb-crrel-dartmouth.org/archived-data/). In this study, we use IMBs deployed in these different regions between 2010-2015 (Fig. 1, Table 1). The IMBs were typically deployed in the Central Arctic during April/May, while deployments in the Beaufort, the Laptev, and Chukchi Seas took place in August/September. For more coverage, we also use snow buoys deployed in 2015 (Table 1; Fig. 1) (http://www.meereisportal.de/en). For simplicity, hereafter we refer to IMBs and Snow Buoys as buoys.

2.2 ERA5 and ERA-I reanalysis data

ERA5 is the ECMWF's latest reanalysis product, and will replace the widely used ERA-I. The first batch of ERA5, covering the period 2010-2016, was released in July 2017. The entire ERA5 dataset, including the period from 1950 to present, is expected to be available for use by early 2019. ERA5 and ERA-I both have global coverage, with a horizontal spatial resolution of 80 km for ERA-I, and 31 km for ERA5. In the vertical, ERA5 resolves the atmosphere using 137 levels from the surface up to a height equalling 0.01 hPa, and ERA-I uses 60 levels from the surface up to an equivalent height of 0.1 hPa. ERA5 provides hourly analysis and forecast fields, while ERA-I provides 6-hourly analysis and 3-hourly forecast fields. For the data assimilation, both apply 4-dimensional variational analysis (4D-var). ERA-I uses the Integrated Forecast System (IFS) "Cy31r2" 4D-Var, and ERA5 applies the newer IFS "Cy41r2" 4D-Var". ERA5 includes various newly reprocessed datasets

and recent instruments that could not be ingested in ERA-I. Many new parameters, such as 100 m wind vector, are available as part of the ERA5 output. For comparison and evaluation, the ERA-I data here are bilinearly interpolated to the grid of the ERA5, and the ERA-I and ERA5 reanalysis are bilinearly interpolated to the buoy positions.

3 Comparison of reanalysis near surface air temperature and precipitation against buoy observations

5 Both ERA-I and ERA5 capture the observed evolution of MSLP measured by each of the buoys (not shown). The hourly difference between the reanalysis MSLP and observations is no more than a few hPa. Excellent agreements between observed MSLP in the Arctic and earlier reanalyses have been shown in previous studies (e.g, Makshtas et al., 2007), demonstrating that MSLP is well simulated in reanalyses.

3.1 Evaluation of near surface temperature in ERA5 and ERA-I using buoy observations

10 Figure 2 and Figure 3 show time series of T2M from different buoys, and the corresponding T2M from ERA5 and ERA-I at the buoys' positions. The observed T2M reveals the pronounced seasonal cycle in the Arctic. Low temperatures persist through winter (January - March) and spring (April - June), before approaching near 0ºC around the end of May or early June. Temperatures near 0ºC, or occasionally over 0ºC, continue during summer (July - September), before lower temperatures return in late August or early September and decrease further in autumn (October - December) (Fig. 2 & 3).

15 The T2M in ERA5 and ERA-I generally agree well, both with each other and the observations (Figs. 2 & 3). The reanalyses perform best for the buoys of 2013E (Fig. 2d), and 2012J (Fig. 3d). However, on occasions, hourly differences of T2M between ERA5 and ERA-I can be up to 8ºC (Fig. 2g and Fig. 3a-c). The largest hourly T2M differences between the two reanalyses, and between the reanalyses and observations, are found during the coldest months (November–May). Specifically, both reanalyses have a warm bias during these months. Previous studies have shown that warm biases in the Arctic are prevalent

20 among most reanalysis products, particularly during the winter season (Beesley et al., 2000; Tjernstöm and Graversen, 2009; Lüpkes et al., 2010; Jacobson et al., 2012; Lindsay et al., 2014; Wesslén et al., 2014; Graham et al., 2017b). This is because weather forecast models and climate models struggle to accurately simulate strong stable boundary layers (Beesley et al., 2000; Tjernstöm and Graversen, 2009; Sotiropoulou et al., 2015; Graham et al., 2017b; Kayser et al., 2017; Biosvert et al., 2018). Interestingly, we find a larger warm bias in the new ERA5 compared with ERA-I (Fig. 2 & 3, Table 2), despite the higher

25 vertical resolution in ERA5.

We note that the near surface air temperature in both reanalyses corresponds to a height of 2 m, while it is typically measured by buoys at a height of about 1.0 m above the surface, when the buoys are installed. The 1.0 m observation height might decrease further as snow accumulates during the cold season. During winter, the lowest temperatures in the Arctic occur under stable conditions with a strong surface-based inversion, meaning that the temperature increases with height from the surface.

30 Hence, the near surface warm bias in reanalyses may partly be attributed to the difference in height with the observations (Vihma et al., 2014).

A scatterplot of the ERA5/ERA-I vs. buoy's T2M clearly reveals the temperature dependence of the warm bias in both reanalyses (Fig. 4a). The data crowd together near the 1:1 line when the air temperature is near 0°C, but spread further above the 1:1 line when the air temperature is low, especially at air temperatures below -25°C. The temperature dependence of the warm bias is also demonstrated in Fig. 4b, which shows the relationship between the daily mean T2M differences with the

5   temperature bins of 5 °C from -45 – +5 °C. When the T2M is below -25 °C, the daily mean difference between reanalysis and observation is more than 2 °C, with ERA5 3.1 – 8.0 °C warmer than in buoys, and ERA-I 2.4 – 4.4 °C warmer (Fig. 4b). For temperature above -25 °C, the bias between reanalysis and buoys is smaller, with ERA5 and ERA-I both 0.75 °C warmer than the observations on average.

Figure 4c shows the bias and standard deviation (std) for the reanalyses for each month, based on the buoy observations,

10   and the temperature difference between the reanalyses. The smallest biases, and the smallest T2M differences between ERA5 and ERA-I are found in the months between July and October (also refer to Fig. 2 & 3). ERA5 is typically warmer than ERA-I (and has a larger warm bias) throughout the winter and spring, including June. However, ERA5 was colder than ERA-I (0.01-0.6 °C), and has smaller biases from July - October (Fig. 4c). Hence, the warm bias in ERA5 is smaller than ERA-I in the warm season (July-October). ERA-I has a warm bias in the warm season, but the bias is smaller (< 0.8°C) compared with that

15   in the cold season (Fig. 4c). Similarly, ERA5 has a small warm bias during July and August (<1°C), and a likely insignificant cold bias (< 0.2°C) in September and October (Fig. 4c).

3.2 Comparison of precipitation and snowfall from ERA5 and ERA-I along buoy drift trajectories

We next compare the cumulative total precipitation and snowfall in ERA5 and ERA-I in autumn and winter, along the drift trajectories of the buoys. We begin accumulating the precipitation from 15 August onwards if the buoy was deployed before

20   this date (Fig. 5), or from 1 October if the buoy was installed after 15 August (Fig. 6). We accumulate the precipitation until 30 April, or the end of operation if the buoy stopped working before 30 April in the respective years (see Table 1).

The accumulated total precipitation in ERA5 is lower than ERA-I for each of the analysed buoys (Figs. 5 & 6, Table 1). On average, the accumulated total precipitation in ERA-I is 19.5 mm water equivalent larger than in ERA5, with difference for the individual buoys ranging from 2.0 (buoy 2012D; Fig. 5c) to 38.4 mm water equivalent (buoy 2011M; Fig. 6a). This is

25   interesting, because ERA-I is known to be a relatively "dry" global reanalysis product in the Arctic compared with most other modern reanalyses (e.g. MERRA-2, CFSR, and JRA-55) (Lindsay et al., 2014; Merkouriadi et al., 2017; Boisvert et al., 2018).

Unlike the accumulated total precipitation, the accumulated snowfall (Sf) in ERA5 can be larger than that in ERA-I (Figs. 5 & 6; Table 1). For buoys deployed near the North Pole, which started operating on 15 August, the accumulated Sf in ERA5 is typically larger than ERA-I. (Fig. 5). In contrast, for buoys deployed in other regions, which started operating on 1 October,

30   the accumulated snowfall in ERA5 is typically lower than ERA-I (Fig. 6). The ratio of snowfall to precipitation in ERA5 is relatively high, meaning that most of the total precipitation falls as snow in ERA5. In contrast, ERA-I has a relatively low snowfall to precipitation ratio, especially during August-September. Hence, substantial precipitation falls as rain in ERA-I

during August-September, while the same precipitation events in ERA5 are classified as snowfall. This explains why the accumulated snowfall in ERA5 is greater than ERA-I for buoys deployed in August, but less than ERA-I for buoys starting in October. The low snowfall to precipitation ratio and large fraction of rainfall in ERA-I is known to be anomalous, and is likely due to the cloud physics scheme used (Dutra et al., 2011). Our findings indicate that ERA5 has significantly less anomalous

5   Arctic rainfall than ERA-I, particularly in August-September (Fig. 5).

Evaluating the performance of precipitation products over the Arctic Ocean is a major challenge due to the lack of observations, and difficulty accurately measuring snowfall (e.g. Lindsay et al., 2014; Rasmussen et al., 2012; Sato et al., 2017; Blanchard-Wrigglesworth et al., 2018; Boisvert et al., 2018; Webster et al., 2018). Here we compare the precipitation from ERA-I and ERA5 with snow depth measurements from the buoys (Table 1). For this comparison, snow depth from the buoys

10 is converted to snow water equivalent (SWE) assuming a mean snow density of 350 kg m^{-3} (Warren et al., 1999). The accumulated total precipitation from ERA5 and ERA-I in Fig. 5 and Fig. 6 is converted to SWE assuming that precipitation falls as snow/solid precipitation when the air temperature is below zero (we call this the accumulated Sp). Caution must be taken here, as the buoys reflect point observations, while the reanalyses provide a grid cell average. Snow depth is known to have large variability even over relatively small spatial scales (Warren et al., 1999; Sturm et al., 2002; Liston et al., 2018). An

15 unknown fraction of the true snow fall will also be lost through blowing snow into leads, which is not accounted for in our calculation below.

The accumulated Sp from ERA-I and ERA5 is typically larger on average 38.9 mm SWE for ERA-I and 26.9 mm SWE for EA5 than the observed SWE, (see Table 1). However, there are cases where the accumulated Sp from both ERA-I and ERA5 was lower (mean: 93.8 mm SWE for ERA-I; 91.6 mm SWE for ERA5) than that from the buoys, which are buoys 2010A,

20 2012D, 2012I and 2015D deployed in the Central Arctic in April except buoy 2012I. For example, along the buoy 2015D, the accumulated Sp from ERA-I (144.4 mm SWE) and ERA5 (140.2 mm SWE) is much lower than that from the buoy (392.0 mm SWE). This may be due to snow drifting up against the buoy structure, or reflect anomalously low precipitation in the reanalyses. In contrast, along the buoy drift trajectory of 2012L which was deployed in Beaufort Sea in late August, the accumulated Sp from ERA-I (76.9 mm SWE) and ERA5 (57.8 mm SWE) is substantially larger than that from the buoy (14.0

25 mm SWE). This might reflect snow erosion or sublimation at the IMB_2012L site, or anomalously high precipitation in the reanalyses.

4 Influence of air temperature and precipitation on sea ice evolution during the freezing season

In this section, we evaluate the impact of different forcing products (ERA-I, ERA5, and the buoys) on sea ice evolution. We focus on the freezing/growth season, from 1 October to 30 April, when sea ice generally starts to grow after summer. This

30 period corresponds to the time when the largest differences of T2M between ERA5 and ERA-I were found (Fig. 2-4). For this exercise, we focus on the buoys of 2011M, 2012H, 2012L, and 2012J that were deployed in late August/early September and operated for more than one year, covering a complete freezing season (Table 1). These buoys were installed either on MYI or

FYI in the central Arctic (buoy 2011M), the Beaufort Sea (buoy 2011M, buoy 2012L), or the Laptev Sea (buoy 2012J). When these buoys were installed, sea ice thickness was usually between 1-2 m, except buoy 2012L (ice thickness of 3.35 m) with a few centimetres of snow (Table 1). We use these buoys to assess the impact of different forcing data on sea ice evolution. For our simple approach we apply an accumulated freezing degree day (FDD) model, which accounts for differences in T2M, and
5   a 1D sea ice model that also account for effects of precipitation.

4.1 Assessing the sea ice evolution with freezing degree days (FDD): impact of temperature bias

Ice growth can be estimated with a freezing degree day (FDD) model. The FDD is defined as the time-integrated air temperature below the seawater freezing point (-1.8 °C) during the freezing season. It is essentially a measure of how cold it has been for how long, reflecting the atmospheric forcing on sea ice mass balance. The thermodynamic ice growth (h), from
10   an initial thickness of 0 m, can be estimated using a simple ice-growth parameterization by Lebedev (Maykut, 1986):

$$h = 1.33 \sum (FDD)^{0.58} \qquad (1)$$

While snow depth is not explicitly expressed in Eq. (1), the relation between h and FDD describes ice growth under an average rate of snow accumulation over the Russian sector of the Arctic Ocean (Maykut, 1986).

When we compare the integrated FDD for the buoys and reanalyses, we find that the FDD is largest for buoys, and smallest
15   for ERA5 (Fig. 7, Table 2). This reflects the warm T2M bias in ERA-I and ERA5, in relation to the buoys, with the largest warm bias in ERA5. The differences in FDD between ERA5, ERA-I and buoys are large for buoys of 2011M, 2012H and 2012L (Fig. 7a-c), but negligible for buoy 2012J (Fig. 7d). Hence the differences in sea ice growth over the freezing season, estimated using FDD from ERA5, ERA-I and buoys, are large for the former but negligible in case of buoy 2012J (Fig. 7). The negative thickness bias in ERA-I with respect to the FDD calculated using the T2M from the buoys ranges from 0.08-0.12
20   m, with a mean of -0.09 m. ERA5 has larger ice thickness biases, ranging from 0.13-0.20 m, with a mean of -0.16 m (Table 2). Hence, the positive near surface air temperature bias in ERA5 and ERA-I results in a negative ice thickness bias at the end of the growth season, when applying this simple FDD model.

4.2 Assessing sea ice evolution with a 1D sea ice model HIGHTSI: impact of T2M and precipitation

HIGHTSI is a 1D high-resolution thermodynamic snow and ice model designed for process studies to accurately resolve the
25   evolution of snow/ice thickness and temperature profile. It has been extensively used in Arctic studies (e.g., Cheng et al., 2008; Cheng et al., 2013; Wang et al., 2015; Merkouriadi et al., 2017).

In this section we perform six sensitivity simulations on each of the four buoys to explore the impact of temperature and precipitation on snow and sea ice evolution (Table 3). In the first two simulations, Sf-ERAI and Sf-ERA5, we force HIGHTSI with the T2M, 10 m wind speed (U10), relative humidity (Rh), total cloud cover (Tcc) and snowfall, from ERA-I and ERA5,
30   respectively. In the next two simulations, Sp-ERAI and Sp-ERA5, we force the model with the total precipitation from the reanalyses, rather than the snowfall, and treat all precipitation as snow when T2M is below 0 °C. This is the same method we

used for the accumulated Sp in section 3.2. In the final two simulations, we evaluate the influences of T2M and precipitation on the sea ice evolution individually. Specifically, we replace the T2M from ERA-I in the Sp-ERAI run with the T2M from ERA5, and name this run T2M-ERA5_Sp-ERAI. Similarly, we replace the Sp from ERA-I, in the run of Sp-ERAI, with the Sp from ERA5 for the T2M-ERAI_Sp-ERA5 run. For all of the simulations we apply the same seasonally variant ocean heat

5   flux according to McPhee et al. (2003). Snow-ice, an ice type formed at ice surface (e.g., Leppäranta, 1983), was recently found to significantly contribute to the Arctic sea ice mass balance in a region with thick snowpack on relatively thin ice pack (Granskog et al., 2017; Merkouriadi et al., 2017). A few (1.5-3) millimetres snow-ice formed only in the Sp-ERAI and T2M-ERA5_Sp-ERAI runs for buoy 2012J (with the lowest initial ice thickness of all buoys examined, Table 1). This is negligible for the total ice mass balance. Thus, the effect we examine solely depends on the differences in T2M and precipitation on

10   thermodynamic ice growth.

The pattern of snow accumulation recorded by many buoys is consistent with observations by Warren et al. (1999). Namely, they record snow accumulation in late fall, followed by a relatively constant snow depth from December/January–March, and sometimes a late increase in snow depth in early spring (Fig. 8). For example, the observed snow depth at buoy 2012H increased to about 0.25 m in late December, and changed marginally thereafter (Fig. 8a). Similarly, the observed snow depth at buoy

15   2012L increased from 0.03 m to 0.13 m from early October to mid-November, and then remained around 0.10 m until the end of April (Fig. 8c). Most buoys recorded an increase in ice thickness from early December to the end of the freezing season. For example, the sea ice growth for buoy 2012H began in early December, at a rate of approximately 0.5 cm/d, until late March, and afterward the growth became sluggish at a rate of 0.16 cm/d until the end of April. However, buoy 2012L, which had an initial ice thickness of ~ 3.3 m, showed no significant growth until early February, before undergoing a slight increase

20   from around 3.3 m to 3.5 m by the end of the freezing season.

We first compare the simulations Sp-ERAI and Sp-ERA5. Differences in the ice thickness at the end of the growth season for the Sp-ERAI and Sp-ERA5 simulations are relatively small, despite the larger warm bias in ERA5 (Fig. 8). In fact, the sea ice was marginally thicker (0.001-0.03 m) in Sp-ERA5 compared with Sp-ERAI for three buoys, and just 0.004 m thinner for buoy 2012L (Fig. 8c). The major differences we see between these simulations is in the snow depth (Figs. 8). Sp-ERAI has a

25   deeper snow pack than Sp-ERA5 for all four buoys, ranging from 0.02-0.09 m. This is due to the higher total precipitation in ERA-I, compared with ERA5 (See section 3.2).

In contrast, when HIGHTSI is forced with the reanalyses snowfall product (Sf-ERAI and Sf-ERA5) the differences in snow depth are relatively small, compared with the simulations forced by the total precipitation (Sp-ERAI and Sp-ERA5). The Sf-ERAI runs typically have a deeper snowpack (on average 0.02 m) than Sf-ERA5. However, the snow depth in Sf-ERAI is

30   thinner (by 0.03 m on average) and ice thickness is greater (about 0.01 m) than the Sp-ERAI runs (Fig. 8). This is because there is substantial rain at sub-zero temperatures in the Sf-ERAI runs that is classified as snow in the Sp-ERAI runs. There are no large differences between the snow depth and sea ice thickness at the end of the growth season for the Sf-ERA5 and Sp-ERA5 runs because, unlike in ERA-I, there is little rain at sub-zero temperatures for Sf-ERA5.

We now look at the effect of T2M differences between ERA5 and ERA-I, and compare the T2M-ERA5_ Sp-ERAI runs vs. Sp-ERAI runs (Fig. 9). When using the T2M from ERA5 and not altering the precipitation forcing, the snowpack remains unchanged from the Sp-ERAI runs. However, we find a slightly thinner ice at the end of freezing season, compared with Sp-ERAI runs (on average 0.01 m thinner), as a result of the larger warm bias in ERA5 which slows down the growth of sea ice.

5 This is consistent with our results from the FDD model in Section 4.1.

Finally, we look at the effect of precipitation by comparing the T2M-ERAI_Sp-ERA5 and Sp-ERAI runs. The snowpack in T2M-EARI_Sp-ERA5 is thinner (on average 0.03 m), while the ice thickness is thicker (on average 0.02 m) than that in the Sp-ERAI runs (Fig. 9). The thinner snowpack, is due to the lower precipitation in ERA5 compared with ERA-I. This thinner snowpack allows more heat loss to the atmosphere, which results in greater ice growth.

10 Referring back to the Sp-ERAI and Sp-ERA5 simulations, we see that lower precipitation and thinner snowpack when using ERA5 as forcing data compensates for the larger T2M warm bias in ERA5, compared with ERA-I. Overall, these compensating biases result in comparable ice thickness at the end of the growth season for both reanalyses.

In general, HIGHTSI reproduces the evolution of snow and sea ice observed by the buoys well during the freezing season (Fig. 8-9) although there are some differences. For the snowpack, there was a 10 cm increase in snow depth for IMB_2012H

15 during late December, which seems not well captured by any of the reanalyses (Fig. 6b) and therefore by any the simulations (Fig. 8a & 9a). The simulations for IMB_2012H show an increase in snow depth at the end of April, indicating a snowfall event in the reanalysis. However, this was not recorded by the buoy. Thus, a good representation of precipitation in the reanalysis data seems crucial for the snow evolution in the simulation, not only the magnitude, but also the frequency of the precipitation. The representation of snow in the model may further influence the simulated ice thickness (e.g., Fig. 8a).

20 Evaluating precipitation in the Arctic is however challenging as mentioned previously due to the large local variability and lack of representative in-situ observations (e.g., Liston et al., 2018). Differences in the modelled sea ice thickness from the buoy observations in part arise from not knowing the local ocean heat flux at each individual buoy, however, our approach is here to look at the sensitivity relative to the differences in T2M and precipitation in the reanalyses.

5. Conclusions

25 Reanalysis data are often used to force snow and sea ice models. The accuracy of these forcing products is paramount for the reproduction of the sea ice evolution in the model. ERA5 is a new global reanalysis product from ECMWF and will replace the widely used ERA-I. Here we compare the 2 m air temperature (T2M) and precipitation in ERA5 and ERA-I, and evaluate these products against in-situ observations from drifting buoys (IMBs and Snow Buoys) over Arctic sea ice.

There is a warm bias in both ERA-I and ERA5 compared with the buoys, which is smallest in summer months, and largest

30 during the autumn, winter and spring. The warm bias in ERA5 is smaller than ERA-I during the summer months. However, we found a larger warm bias in ERA5 than ERAI during the cold season, especially when the observed T2M was lower than -25 °C. For days when the observed T2M was <-25 °C, the daily mean difference between the reanalyses and buoys was, on

average, +5.4 °C for ERA5 and +3.4 °C for ERA-I. The larger warm bias in ERA5 during cold periods indicates this reanalyses still struggles to accurately simulate strong stable boundary layers, which frequently appear in winter and early spring, despite the higher vertical resolution compared with ERA-I (e.g., Beesley et al., 2000). Nonetheless, in the summer months, the warm bias in ERA5 (less than 0.2 °C) was smaller than ERA-I.

5   The total precipitation in ERA5 was lower than in ERA-I along the buoy drift trajectories. This is surprising, as ERA-I is known to be drier in the Arctic compared with other recent reanalyses (Lindsay et al., 2014; Merkouriadi et al., 2017; Boisvert et al., 2018). ERA-I has an anomalously large fraction of liquid precipitation in the Arctic, especially during August-September (Dutra et al., 2011), which is not present in ERA5. The snowfall component of precipitation are in better agreement between the two reanalyses than the total precipitation. The accumulated solid precipitation (Sp) in ERA5 is often closer to the SWE

10   content of buoy snow pack, compared with ERA-I. However the lack of representative in-situ observations and difficulty in measuring snow accumulation on sea ice in the Arctic makes it a challenge to accurately evaluate precipitation products over sea ice (e.g. Rasmussen et al., 2012; Lindsay et al., 2014; Sato et al., 2017; Blanchard-Wrigglesworth et al., 2018; Boisvert et al., 2018). Nonetheless, snow is a critical factor in sea ice evolution and therefore more representative observations are needed (e.g. Merkouriadi et al., 2017; Webster et al., 2018).

15   The larger warm bias during the ice growth season in ERA5, compared with ERA-I, can result in a lower ice thickness when using this as a forcing product for an ice model or a FDD model. However, this bias is compensated by the lower precipitation in ERA5, which results in a thinner snow pack that allows more heat loss to the atmosphere. Overall, using a 1D thermodynamic sea ice model simulations with ERA5 had a slightly larger ice thickness compared with ERA-I at the end of the growth season, despite the larger warm bias in ERA5. Compared with the T2M differences between the two reanalyses,

20   precipitation differences had a greater influence on the snow and ice evolution. More precipitation / snow data on sea ice are clearly required to properly evaluate reanalyses precipitation in the central Arctic.

Authors contributions

CW, KW and MAG initiated the study. CW and MAG retrieved the buoy data. CW and KW downloaded and analysed the reanalysis data and performed the 1D model simulations. All authors contributed to writing the manuscript.

25   **Acknowledgements**

This study was supported by the Research Council of Norway through project SPARSE (project 254765), the Fram Centre "Arctic Ocean" flagship program through the SOLICE project, and by the Centre for Ice, Climate and Ecosystems (ICE) at the Norwegian Polar Institute through the N-ICE project. We wish to acknowledge ECMWF for ERA-Interim and ERA5 data, the International Arctic Buoy Program (IABP) for the IMB data (http://imb-crrel-dartmouth.org/results/), and the Alfred Wegener

30   Institute for Snow Buoy data (http://data.seaiceportal.de/gallery/index_new.php).

References

Albergel, C., Dutra, E., Munier, S., Calvet, J.-C., Munoz-Sabater, J., Rosnay, P., and Balsamo, G.: ERA-5 and ERA-Interim driven ISBA land surface model simulations: which one performs better? Hydol. Earth Syst. Sci, 22, 3515-3532, doi.org/10.5194/hess-22-3515-2018, 2018.

5 Alexeev, V. A., Walsh, J. E., Ivanov, V. V., Semenov, V. A., and Smirnov, A. V.: Warming in the Nordic Seas, North Atlantic storms and thinning Arctic sea ice, Environmental Res. Lett., 12, 084011, 2017.

AMAP, Snow, Water, Ice and Permafrost in the Arctic (SWIPA) 2017. Arctic Monitoring and Assessment Programme (AMAP), Oslo, Norway, Xiv +269 pp, 2017.

Beesley, J. A., Bretherton, C. S., Jakob C., Anderas, E. L., Intrieri, J. M., and Uttal, T. A.: A comparison of cloud and boundary
10   layer variables in the ECMWF forecast model with observations at Surface Heat Budget of the Arctic Ocean (SHEBA) ice camp, J. Geophys. Res., 105(D10), 12337-12349, doi:10.1029/2000JD900079, 2000.

Bekryaev, R. V., Polyakov, I. V., and Alexeev, V. A.: Role of polar amplification in long-term surface air temperature variations and modern arctic warming, J. Clim., 23(14), 3888–3906, doi:10.1175/2010JCLI3297.1, 2010.

Blanchard-Wrigglesworth, E., Webster, M. A., Farrell, S. L., and Bitz, C. M.: Reconstruction of snow on Arctic sea ice, J.
15   Geophys. Res., Oceans, 123, 3588-3602, https://doi.org/10.1002/2017JC013364, 2018.

Boisvert, L. N., and Stroeve, J. C.: The Arctic is becoming warmer and wetter as revealed by the Atmospheric Infrared Sounder. Geophys. Res. Lett., 42, 4439–4446, doi:10.1002/2015GL063775, 2015.

Boisvert, L. N., Webster, M. A.,Petty, A. A., Markus, T., Bromwich, D. H., and Cullather R. I.:: Intercomparison of precipitation estimates over the Arctic Ocean and its peripheral seas from reanalyses, J. Clim., doi:10.1175/JCLI-D-18-
20   0125.1, 2018.

Cheng, B., Zhang, Z., Vihma, T., Johansson, M., Bian, L., Li, Z., and Wu, H.: Model experiments on snow and ice thermodynamics in the Arctic Ocean with CHINARE 2003 data, J. Geophys. Res., 113, C09020, doi: 10.1029/2007JC004654, 2008.

Cheng, B., Mäkynen, M., Similä, M., Rontu, L., and Vihma, T.: Modelling snow and ice thickness in the coastal Kara Sea,
25   Russia Arctic, Ann. Glaciol., 54(62), doi:10.3189/2013AoG62A180, 2013.

Comiso, J. C., Parkinson, L., Gersten, R., and Stock, L.: Accelerated decline in the Arctic sea ice cover, Geophys. Res.Lett., 35, L01703, doi10.1029/2007GL031972, 2008.

Dahlke, S., and Maturilli, M.: Contribution of Atmospheric Advection to the Amplified Winter Warming in the Arctic North Atlantic Region, Advances in Meteorol., doi:10.1155/2017/4928620, 2017.

30 Decker, M., Brunke, M. A., Wang, Z., Sakguchi, K., Zeng, X., and Bosilovich, M. G.: Evaluation of the reanalysis products from GSFC, NCEP, and ECMWF using flux tower observations, J. Clim., 25, 1916-1944, doi:10.1175/JCLI-D-11-00004.1, 2012.

Dee, D. P., Uppala, S. M., Simmons, A. J., Berrisford, P., Poli, P., Kobayashi, S., Andrae, U., Balmaseda, M. A., Balsamo, G., Bauer, P., Bechtold P., Beljaars, A. C. M., Berg, L. van de, Bidlot, J., Bormann, N., Delsol, C., Dragani, R., Fuentes, M., Geer, A. J., Haimberger, L., Healy, S. B., Hersbach, H., Hólm, E. V., Isaksen, L., Kållberg, P., Köhler, M., Matricardi, M., McNally, A. P., Monge-Sanz, B. M., Morcrette, J.-J., Park, B.-K., Peubey, C., Rosany, P. de, Tavolato, C., Thépaut, J.-N., and Vitart, F.: The ERA-Interim reanalysis: configuration and performance of the data assimilation system, Quart. J. Roy. Meteor. Soc., 137, 553-597, 2011.

Dutra, E., Schär, C., Viterbo, P., and Miranda, P. M. A.: Land-atmosphere coupling associated with snow cover, Geophys. Res. Lett., 38, L15707, doi:10.1029/2011GL048435, 2011.

Graham, R. M., Cohen, L., Petty, A. A., Boisvert, L. N., Rinke, A., Hudson, S. R., Nicolaus, M., and Granskog, M. A.: Increasing frequency and duration of Arctic winter warming events, Geophys. Res. Lett., 44, 6974-6983, doi:10.1002/2017GL073395, 2017a.

Graham, R. M., Rinke, A., Cohen, L., Hudson, S. R., Walden, V. P., Granskog, M. A., Dorn, W., Kayser, M., and Maturilli, M.: A comparison of the two Arctic atmospheric winter states observed during N-ICE2015 and SHEBA, J. Geophys. Res., Atmos., 122, 5716-5737, doi:10.1002/2016JD025475, 2017b.

Granskog, M. A., Rösel, A., Dodd, P. A., Divine, D., Gerland, S., Martma, T., and Leng, M. J.: Snow contribution to first-year and second-year Arctic sea ice mass balance north of Svalbard, J. Geophys. Res., Oceans, 122, 2539-2549, doi:10.1002/2016JC012398, 2017.

Graversen, R. G., Mauritsen, T., Tjernström, M., Källén, E., and Svensson, G.: Vertical structure of recent Arctic warming, Nature, 451(7174), 53-56, doi:10.1038/nature06502, 2008.

Grosfeld, K. Treffeisen, R., Asseng, J., Bartsch, A., Bräuer, B., Fritzsch, B., Gerdes, R., Hendricks, S., Hiller, W., Heygster, G., Krumpen, T., Lemke, P., Melsheimer, C., Nicolaus, M., Ricker, R., and Weigelt, M.: Online sea-ice knowledge and data platform <www.meereisportal.de>, Polarforschung, Bremerhaven, Alfred Wegener Institute for Polar and Marine Research and German Society of Polar Research, 85(22), 143-155, doi:10.2312/polfor.2016.011, 2016.

Jakobson, E., Vihma, T., Palo, T., Jakobson, L., Keernik, H., and Jaagus, J.: Validation of atmospheric reanalyses over the central Arctic Ocean, Geophys. Res. Lett., 39(10), L10802, doi:10.1029/2012GL051591, 2012.

Kapsch, M. L., Graversen, R. G., Economou, T., and Tjernström, M.: The importance of spring atmospheric conditions for predictions of the Arctic summer sea ice extent, Geophys. Res. Lett., 41, 5288–5296, doi:10.1002/2014GL060826, 2014.

Kayser, M., Maturilli, M., Graham, R. M., Hudson, S. R., Rinke, A., Cohen, L., Kim, J.-H., Park, S.-J., Moon, W., Granskog, M. A.: Vertical thermodynamic structure of the troposphere during the Norwegian young sea ICE expedition (N-ICE2015), J. Geophys. Res., Atmosphere, 122(20), doi:10.1002/2016JD026089, 2017.

King, J., Spreen, G., Gerland, S., Haas, C., Hendriks, S., Kaleschke, L., and Wang, C.: Sea-ice thickness from field measurements in the northwestern Barents Sea, J. Geophys. Res. Oceans, 122, 1497-1512, doi:10.1002/2016J012199, 2018.

Hersbach, H., and Dee., D: ERA5 reanalysis is in production, ECMWF Newsletter 147, ECMWF, http://ww.ecmwf.inten/elibrary/16299-newsletter-nol47-spring%g-2016 (last access: 24 March 2017), 2016.

Launiainen, J., and Cheng, B.: Modelling of ice thermodynamics in natural water bodies, Cold Reg. Sci. Technol., 27, 153-178, 1998.

5   Leppäranta, M.: A growth model for black ice, snow ice and snow thickness in subarctic basins, Hydro. Res., 14(2), 59-70, 1978.

Lindsay, R., and Schweiger, A.: Arctic sea ice thickness loss determined using subsurface, aircraft, and satellite observations. TC, 9(1), 269–283, doi:10.5194/tc-9-269-2015, 2015.

Lindsay, R., Wensnahan, M., Schweiger, A., and Zhang, J.: Evaluation of seven different atmospheric reanalysis products in

10   the Arctic, J. Clim., 27(7), 2588–2606, doi:10.1175/JCLI-D-13-00014, 2014.

Liston, G. E., Polashenski, C., Rösel, A., Itkin, P., King, J., Merkouriadi, I., and Haapala, J.,: A distributed snow-evolution model for sea-ice applications (SnowModel), J. Geophys. Res., Oceans, 123, 3786-3810. https://doi.org/10.1002/2017JC013706, 2018.

Lüpkes, C., Vihma, T., Jakobson, E., König-Langlo, G., and Tetzlaff, A.: Meteorological observations from ship cruises during

15   summer to the central Arctic: A comparison with reanalysis data, Geophys. Res. Lett., 37(9), 850, doi:10.1029/2010GL042724, 2010.

Makshtas, A., Atkinson, D., Kulakov, M., Shutilin, S., Krishfield, R., and Proshutinsky, A.: Atmospheric forcing validation for modeling the central Arctic, Geophys. Res. Lett., 34, L20706, doi:10.1029/2007GL031378, 2007.

Maksimovich, E., and Vihma, T.: The effect of surface heat fluxes on interannual variability in the spring onset of snow melt

20   in the central Arctic Ocean, J. Geophys. Res., 117, C07012, doi:10.1029/2011JC007220, 2012.

Markus, T., Stroeve, J. C., and Miller J.: Recent changes in Arctic sea ice melt onset, freezeup, and melt season length, J. Geophys. Res., 114, C12024, doi:10.1029/2009JC005436, 2009.

Maslanik, J., Stroeve, J., Fowler, C., and Emery, W.: Distribution and trends in Arctic sea ice age through spring 2011, Geophys. Res. Lett., 38, L13502, doi:10.1029/2011GL047735, 2011.

25   Maykut, G. A.: The surface heat and mass balance, in Geophysics of Sea Ice, edited by N. Untersteiner, pp. 395–463, Plenum, New York, 1986.

Merkouriadi, I., Cheng, B., Graham, R. M., Rösel, A., and Granskog, M. A.: Critical Role of Snow on Sea Ice Growth in the Atlantic Sector of the Arctic Ocean, Geophys. Res. Lett., 44(20), doi:10.1002/2017GL075494, 2017.

Mortin, J., Graversen, R. G., and Svensson, G.:. Evaluation of pan-Arctic melt-freeze onset in CMIP5 climate models and

30   reanalyses using surface observations, Clim. Dyn., 42, 2239–2257, doi:10.1007/s00382-013-1811-z, 2014.

Mortin, J., Svensson, G., Graversen, R. G., Kapsch, M. L., Stroeve, J. C., and Boisvert, L. N.: Melt onset over Arctic sea ice controlled by atmospheric moisture transport, Geophys. Res. Lett., 43(12), 6636–6642, doi:10.1002/2016GL069330, 2016.

Nicolaus, M., Hoppmann, M., Arndt, S., Hendricks, S., Kaltein, C., König-Langlo, G., Nicolaus, A., Rossmann, L., Schiller, M., Schwegmann, S., Langevin, D., Bartsch, A.: Snow height and air temperature on sea ice from snow buoy measurements, Alfred Wegener Institute, Helmholtz Center for Polar and Marine Research, Bremerhaven, PANGAEA, doi:0.1594/PANGAEA.875638, 2017.

5   Olauson, J.: ERA5: The new champion of wind power modelling? Renew. Energy, 126, 322-331, doi.org/10.1016/j.renene.2018.03.056, 2018.

Perovich, D., Richter-Menge, J., and Polashenski, C.: Observing and understanding climate changes: Monitoring the mass balance, motion, and thickness of Arctic sea ice, http://imb.crrel-datmouth.org, 2018.

Polashenski, C., Perovich, D., Richter-Menge, J., and Elder, B.: Seasonal ice mass-balance buoys: adapting tools to the

10   changing Arctic, Ann. Glaciol., 52(57), 18- 26, 2011.

Polyakov, I. V., Timokhov, L. A., Alexeev, V. A., Bacon, S., Dimtrenko, I. A., Fortier L, Frolov, I. E., Gascard, J.-C., Hansen, E., Ivanov, V. V., Laxon, S., Mauritzen, C., Perovich, D., Shimada, K., Simmons, H. L., Sokolov, V. T., Steele, M., and Toole, J.: Arctic ocean warming contributes to reduced polar ice cap, J. Phys. Oceanogr., 40, 2743-2756, 2010.

Rasmussen, R., Baker, B., Kochendorfer, J., Meyers, T., Landolt, S., Fischer, A. P., Black, J., Thériault, J. M., Kucera, P.,

15   Gochis, D., Smith, C., Nitu, R., Hall, M., Ikeda, K., and Gutmann, E.: How well are we measuring snow: The NOAA/FAA/NCAR winter precipitation test bed, Bull. Amer. Meteor. Soc., 93, 811- 829, doi: 10.1175/BAMS-D-11-00052.1, 2012.

Richter-Menge, J., Perovich, D. K., Elder, B. C., Claffey, K., Rigor, I., and Ortmeyer M.: Ice mass balance buoys: a tool for measuring and attributing changes in the thickness of the Arctic sea ice cover, Ann. Glaciol., 44, 205-210, 2006.

20   Rigor, I. G., Colony, R. L., and Martin, S.: Variations in Surface Air Temperature Observations in the Arctic, 1979 – 97, J. Clim., 13, 896–914, 2000.

Rinke, A., Maturilli, M., Graham, R. M., Matthes, H., Handorf, D., Cohen, L., Hudson, S. R., and Moore J. C.: Extreme cyclone events in the Arctic: Wintertime variability and trends, Environ. Res. Lett., 12(9), doi:10.1088/1748-9326/aa7def, 2017.

Sato, K., and Inoue, J.: Comparison of Arctic sea ice thickness and snow depth estimates from CFSR with in situ observations,

25   Clim. Dyn., 50(1), 1–13, doi:10.1007/s00382-017-3607-z, 2017.

Schweiger, A., Lindsay, R., Zhang, J., Steele, M., Stern, H., and Kwok, R.: Uncertainty in modeled Arctic sea ice volume, J. Geophys. Res., Ocean, 116(9), 1–21, doi:10.1029/2011JC007084, 2011.

Screen, J. A., and Simmonds, I.: The central role of diminishing sea ice in recent Arctic temperature amplification, Nature, 464(7293), 1334–1337, doi:10.1038/nature09051, 2010.

30   Sotiropoulou, G., Sedlar, J., Forbes, R., and Tjernström, M.: Summer Arctic clouds in the ECMWF forecast model: An evaluation of cloud parameterization schemes, Quart. J. Roy. Meteor. Soc., 142, 387-400, doi:10.1002/qj.2658, 2015.

Steel, M., Ermold, W., and Zhang, J.: Arctic ocean surface warming trends over the past 10 years, Geophys. Res. Lett., 35, L02614, doi:10.1029/98GL00251, 2008.

Stroeve, J., and Notz D.: Chaning state of Arctic sea ice across all the seasons, Env. Res. Lett., 13, 103001, https://doi.org/10.1088/1748-9326/aade56, 2018.

Stroeve, J. C., Serreze, M. C., Holland, M. M., Kay, J. E., Malanik, J., and Barrett A. P.: The Arctic's rapidly shrinking sea ice cover: A research synthesis, Clim. Change, 110(3-4), 1005–1027, doi:10.1007/s10584-011-0101-1, 2012.

5   Stroeve, J. C., Markus, T., Boisvert, L., Miller, J., and Barrett, A.: Changes in Arctic melt season and implications for sea ice loss, Geophys. Res. Lett., 41, 1216-1225, doi:10.1002/2013GL058951, 2014.

Stroeve, J., Schroder, D., Tsamados, M., and Feltham, D.: Warm Winter, Thin Ice? The Cryosphere, 1791–1809, doi:10.5194/tc-12-1791-2018, 2018.

Sturm, M., Holmgren, J., and Perovich, D. K.: Winter snow cover on the sea ice of the Arctic Ocean at the Surface Heat Budget

10   of the Arctic Ocean (SHEBA): Temporal evolution and spatial variability, J. Geophys. Res., 107(C10), 8047, doi:10.1029/2000JC000400, 2002.

Tjernstöm, M., and Graversen, R. G: The Vertical Structure of the lower Arctic troposphere analysed from observations and the ERA-40 reanalysis, Quart. J. Roy. Meteor. Soc., 135, 431-443, doi:10.1002/qj.380, 2009.

Urraca, R., Huld, T., Gracia-Amillo, A., Martinez-de-Pison, F. J., Kaspar, F., and Sanz-Garcia, A.: Evaluation of global

15   horizontal irradiance estimates from ERA5 and COSMO-REA6 reanalysis using ground and satellite-based data, Sol. Energy, 164, 339-354, doi.org/10.1016/j.solener.2018.02.059, 2018.

Vihma, T., Pirazzini, R., Fer, I., Renfrew, I. A., Sedlar, J., Tjernström, M., Lüpkes, C., Nygård, T., Notz, D., Weiss, J., Marsan, D., Cheng, B., Birnbaum, G., Gerland, S., Chechin, D., and Gascard, J. C..: Advances in understanding and parameterization of small-scale physical processes in the marine Arctic climate system: a review, Atmos. Chem. Phys., 14, 9403-9450,

20   www.atmos-chem-phys.net/14/9403/2014/, doi:10.5194/acp-14-9403-2014, 2014.

Wang, C., Shi, L., Gerland, S., Granskog, M. A., Renner, A. H. H., Li, Z., Hansen, and Martma, T.: Spring sea-ice evolution in Rijpfjorden (80° N), Svalbard, from in-situ measurements and ice mass-balance buoy (IMB) data, Ann. Glacio., 54(62), doi:10.3189/2013AoG62A135, 2013.

Wang, C., Cheng, B., Wang, K., Gerland, S., and Pavlova O.: Modelling snow ice and superimposed ice on landfast sea ice in

25   Kongsfjorden, Svalbard, Polar Res., 34, 20828, http://dx.doi.org/10.3402/polar.v34.20828, 2015.

Warren, S. G., Rigor, I. G., Untersteiner, N., Radionov, V. F., Bryazgin, N. N., Aleksandrov, Y. I., and Colony, R.: Snow depth on Arctic sea ice, J. Clim., 12, 1814-1829, 1999.

Webster, M., Gerland, S., Holland, M., Hunke, E., Kwok, R., Lecomte, O., Massom, R., Perovich, D., and Sturm, M.: Snow in the changing sea-ice systems, Nat. Clim. Change, doi.org/10.1038/s41558-018-0286-7, 2018.

30   Wesslén, C., Tjernström, M., Bromwich, D. H., De Boer, G., Ekman, A. M. L., Bai, L. S., and Wang, S. H.: The Arctic summer atmosphere: An evaluation of reanalyses using ASCOS data, Atmos. Chem. Phys., 14(5), 2605–2624, doi:10.5194/acp-14-2605-2014, 2014.

Woods, C., and Caballero R.: The role of moist intrusions in winter Arctic warming and sea ice decline, J. Clim., 29, 4473-
    4485, doi:10.1175/JCLI-D-15-0773.1, 2016.

Table 1. Summary of deployment locations and initial conditions for the buoys. The accumulated snow water equivalent (SWE) is given based on ERA-I, ERA5 and buoy data. The cumulative SWE solid precipitation (Sp) is based on total precipitation assuming precipitation falls as snow when T2M is <0 °C. The cumulative snowfall (Sf) is calculated in the same period as what did for Sp. The accumulated SWE measured by the buoy is assuming a snow density of 350 kg m^{-3}.

Buoy	Deployment location	Period of operation	Ice type	Initial thickness (m)		Accumulated SWE (mm water equivalent)				
						ERA-I		ERA5		Buoy
				ice	snow	Sp	Sf	Sp	Sf	SWE
2010A	Central Arctic	20 Apr 2010 – 2 Dec 2010	FYI	1.67	0.24	77.5[B]	51.8 [B]	71.8 [B]	70.7[B]	84.0[B]
2011M	Central Arctic	29 Sept 2011 – 22 Apr 2013	MYI	1.67	0.07	94.6[A]	89.2 [A]	56.2 [A]	56.2[A]	56.0[A]
2012C	Central Arctic	13 Apr 2012 - 4 Oct 2012	FYI	1.24	0.43	56.2[B]	21.1 [B]	26.2 [B]	22.9[B]	NA
2012D	Central Arctic	4 May 2012 - 2 Nov 2012	FYI	1.67	0.47	89.9[B]	47.1 [B]	86.9 [B]	77.3[B]	161.0 [A]
2012H	Beaufort Sea	10 Sept 2012 - 16 Jan 2014	FYI	1.50	0.02	75.8[A]	68.1 [A]	46.7 [A]	46.7[A]	70.0[A]
2012L	Beaufort Sea	27 Aug 2012 - 25 Sept 2013	MYI	3.35	0.02	76.9[A]	69.3 [A]	57.8 [A]	57.7[A]	14.0[A]
2012I	Chukchi Sea	14 Aug 2012 - 21 Dec 2012	MYI	1.09	0.10	94.8[B]	71.1 [B]	85.7 [B]	80.0[B]	119.0[B]
2012J	Laptev Sea	25 Aug 2012 – 11 Jan 2014	MYI	1.09	0	80.3[A]	71.2 [A]	60.5 [A]	60.5[A]	52.5[A]
2013B	Central Arctic	10 Apr 2013 - 19 Dec 2013	NA	2.00	0.02	151.3[B]	104.0 [B]	135.5 [B]	117.5[B]	84.0[B]
2013E	Central Arctic	11 Apr 2013 - 4 Oct 2013	FYI	1.40	0.05	57.4[B]	17.8 [B]	37.7	35.1[B]	NA
2013H	Central Arctic	3 Sept 2013 - 29 Dec 2013	NA	1.30	0.05	42.3[C]	38.3 [C]	34.7 [C]	34.7[C]	17.5[C]
2014E	Central Arctic	11 Apr 2014 - 18 Feb 2015	NA	1.73	0.19	182.6[B]	122.9 [B]	156.1 [B]	145.7[B]	140.0[B]
2015D	Central Arctic	10 Apr 2015 - 1 Feb 2016	NA	1.96	0.05	144.4[C]	110.7 [C]	140.2 [C]	136.7[C]	392.0[C]
s16	Laptev Sea	19 Sept 2015 - 20 Dec 2016	FYI	NA	0.07	123.6[A]	107.6 [A]	105.8 [A]	105.8[A]	91.0[A]
s20	Central Arctic	14 Sept 2015 – 19 Apr 2016	FYI	1.50	0.05	84.0[C]	76.8 [C]	54.3 [C]	54.2[C]	35.0[C]
s29	Laptev Sea	10 Sept 2015 - 16 Oct 2016	FYI	1.20	0.01	108.5[A]	95.9 [A]	85.0 [A]	84.9[A]	70.0[A]

5   NA: no data

[A]: from 1 October to 30 April.

[B]: from 15 August until the IMB fails or there is no snow data.

[C]: from 1 October until the buoy fails or there is no longer snow data during the first freezing season

Table 2. The mean T2M, accumulated FDD, and estimated ice growth with FDD model

Buoy	T2M mean (°C)			FDD (K·d)[A] /ice growth (m)[B]		
	ERA5	ERA-I	Buoy	ERA5	ERA-I	Buoy
2011M	-22.5	-24.2	-26.6	4295/1.70	4662/1.78	5174/1.90
2012H	-22.5	-24.1	-25.8	4276/1.70	4624/1.78	4978/1.85
2012L	-22.1	-23.1	-24.9	4198/1.68	4402/1.73	4788/1.81
2012J	-20.8	-20.8	NA	4198/1.68	4402/1.72	NA

NA: no data

[A]: from 1 October to 30 April.

[B]: ice growth estimation by the end of freezing season with the Lebedev FDD model (Maykut, 1986).

Table 3. Atmospheric forcing data in model simulations, where U10 is wind at 10 m height (U10), Rh is relative humidity (Rh), and Tcc is total cloud cover (Tcc).

Model runs	T2M	Precipitation	U10, Rh, Tcc
Sp-ERAI	ERA-I	Sp from ERA-I	ERA-I
Sp-ERA5	ERA5	Sp from ERA5	ERA5
Sf_ERAI	ERA-I	Sf from ERA-I	ERA-I
Sf_ERA5	ERA5	Sf from ERA5	ERA5
T2M-ERA5_Sp-ERAI	ERA5	Sp from ERA-I	ERA-I
T2M-ERAI_Sp-ERA5	ERA-I	Sp from ERA5	ERA-I
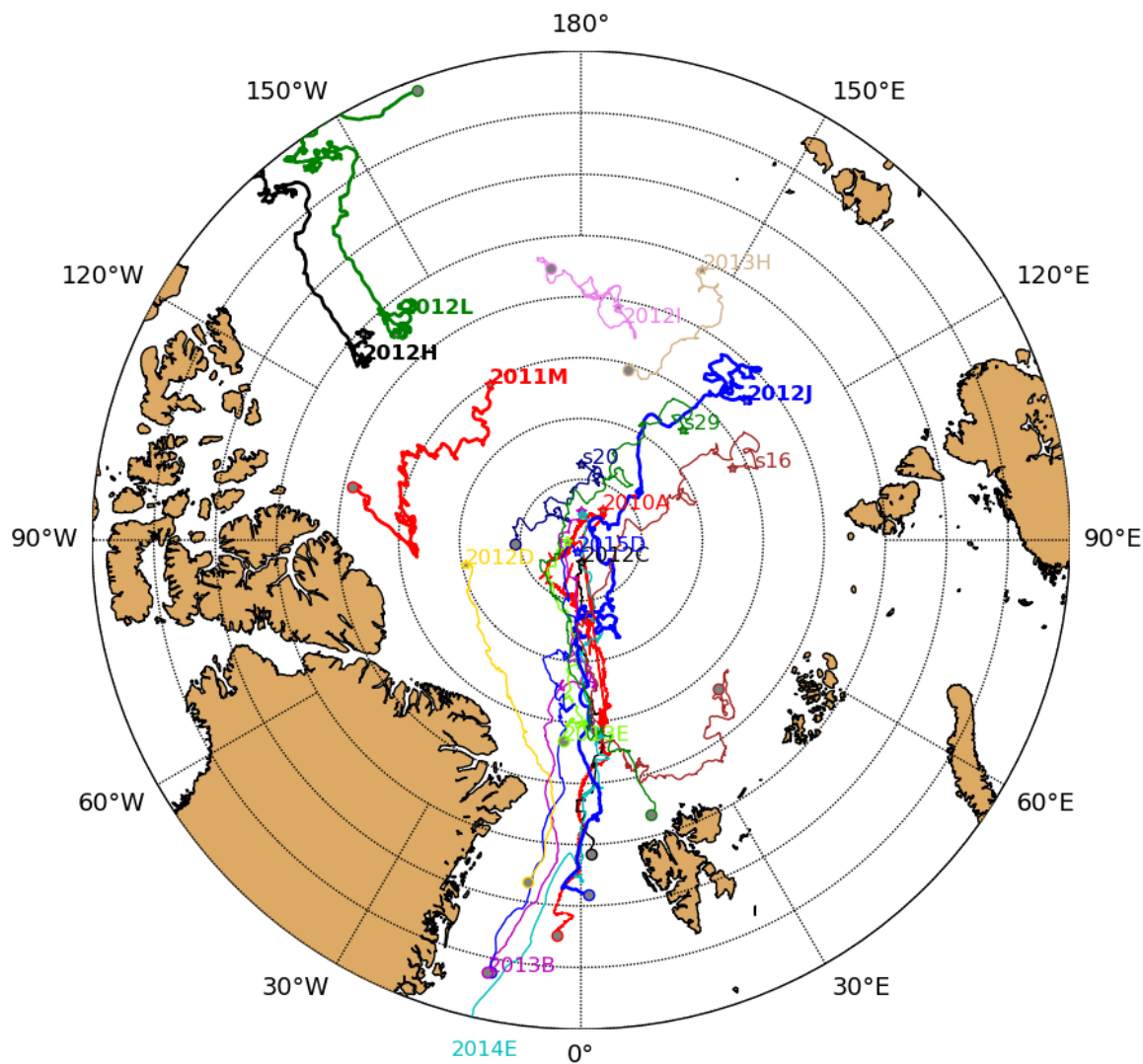
Figure 1. Drift trajectories of all the selected buoys (IMBs and snow buoys). Symbol "⋆" indicates the start of the drift and "o" signals the end of the drift. Buoys' names are labelled at the beginning or the end of the drift using same colour as lines. Buoys used for model simulations are highlighted with solid thick line and bold font.
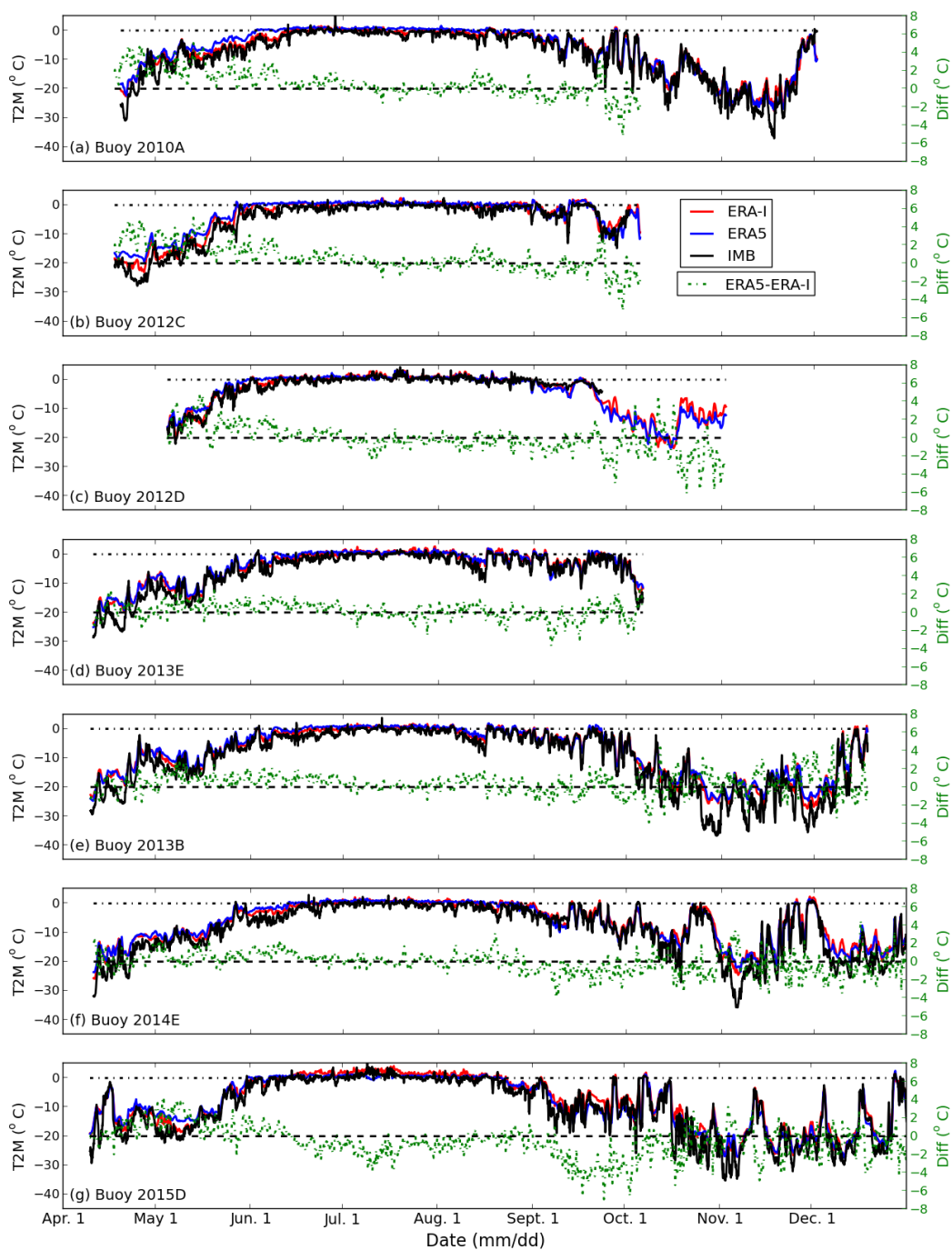
Figure 2. Variation of 2 m air temperature (T2M) in ERA5, ERA-I and the buoys (left side y-axis) and the differences of T2M between ERA5 and ERA-I (right side green y-axis) for buoys deployed in April.
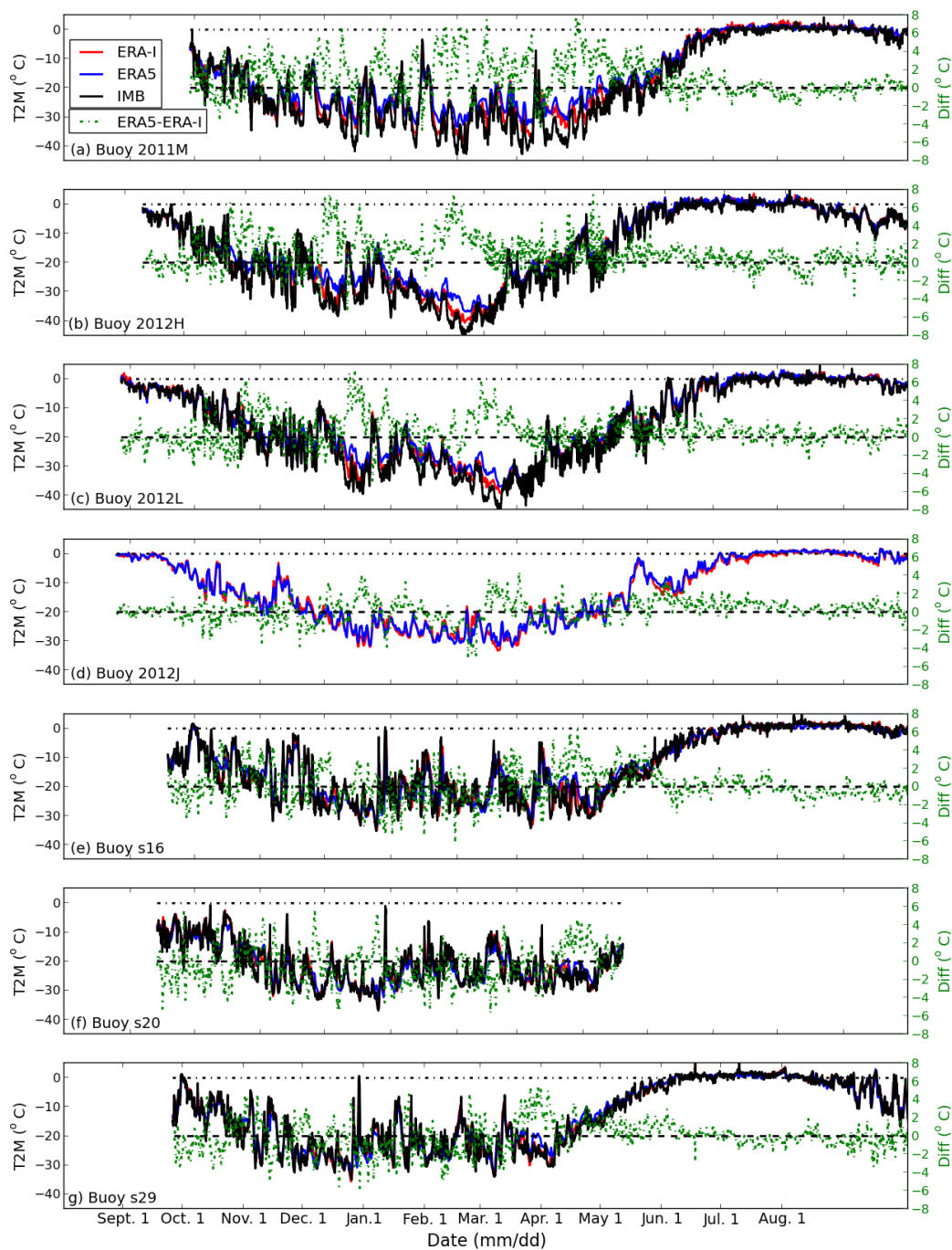
Figure 3. Same as Figure 2, but for buoys deployed from September-October. There is no black line in panel (k) due to no observational data.
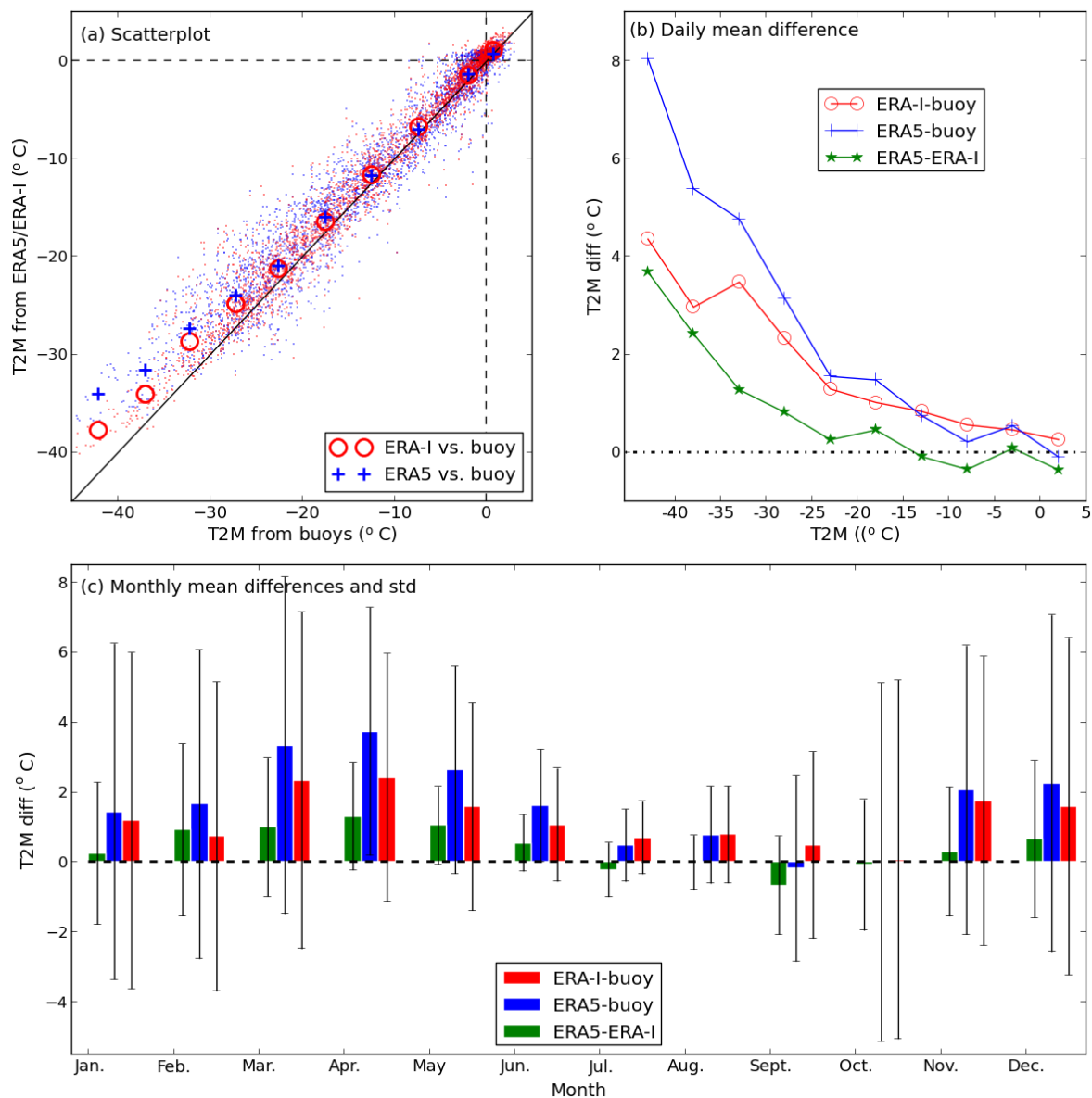
Fig. 4. Statistics of T2M from ERA5, ERA-I and all the buoys. (a) Scatter plot for all data (small dots) and average T2M at 5 degree bins between -45 °C and +5 °C, (b) Daily temperature differences between the reanalysis and between the reanalysis and the buoys corresponding to 5 degree bins between -45 °C and +5 °C, and (c) monthly mean differences and standard deviation (std). In panel

5 **a, the black solid line is for 1:1.**
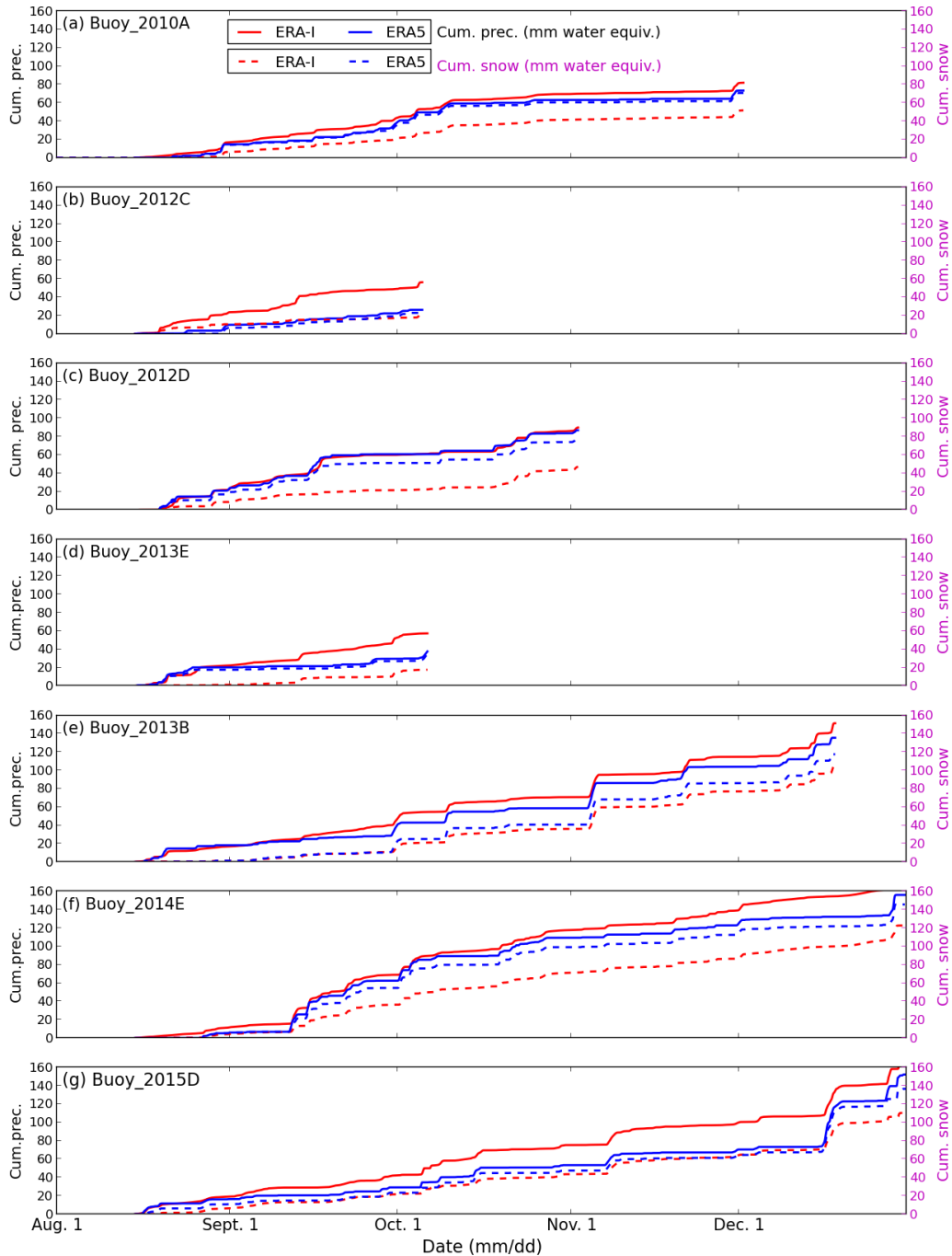
Figure 5. Cumulative total precipitation (left side y-axis) and snowfall (right side magenta y-axis) with accumulation starting from 15 August. Red lines are for ERA-I, and blue lines are for ERA5, with solid lines for the cumulative total precipitation, and dashed lines for the cumulative snowfall.
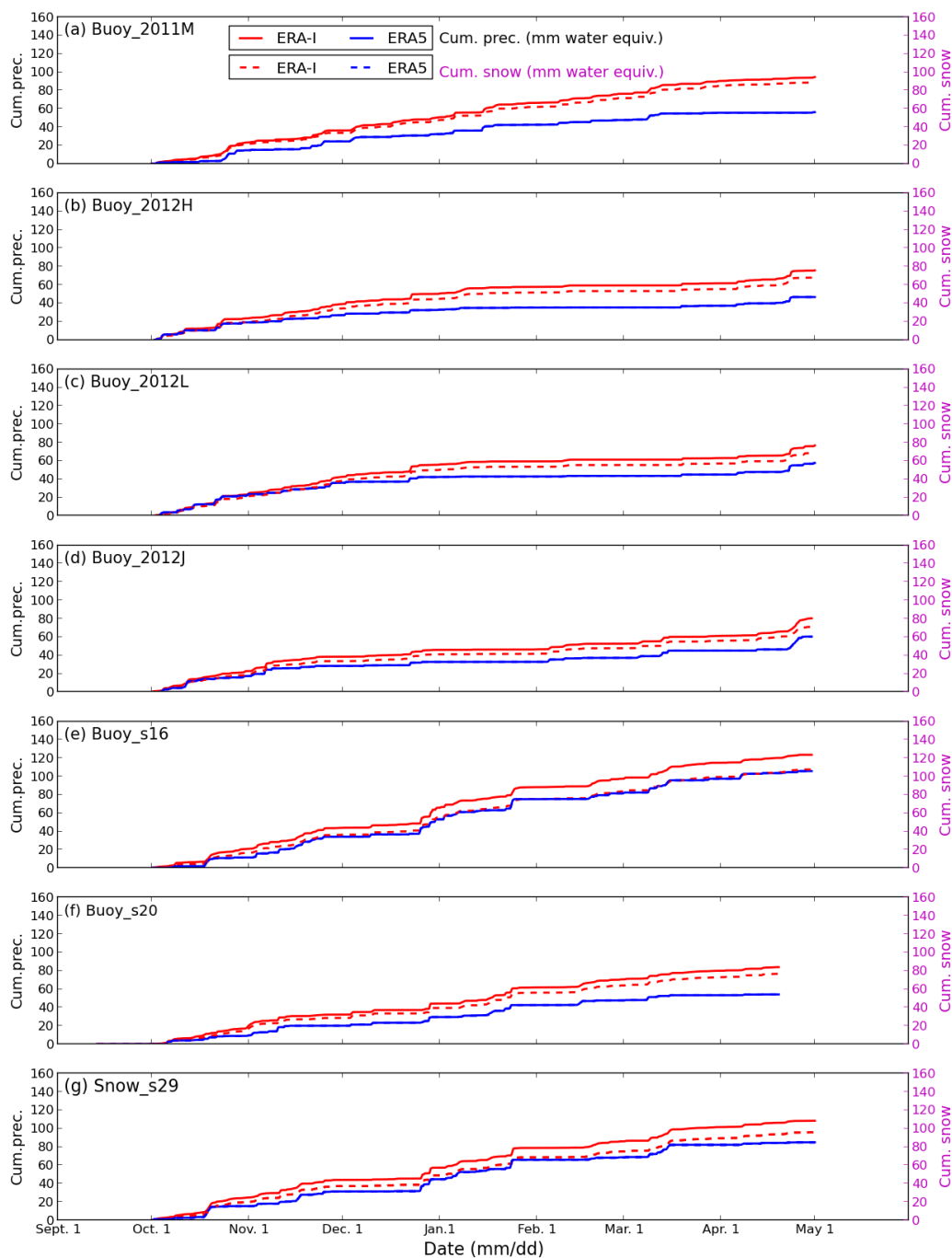
Figure 6. Same as Figure 5, but with accumulation starting from 1 October. The dashed blue lines overlap with the solid blue lines in the panels due to the small differences between the cumulative total precipitation and snowfall in ERA5.
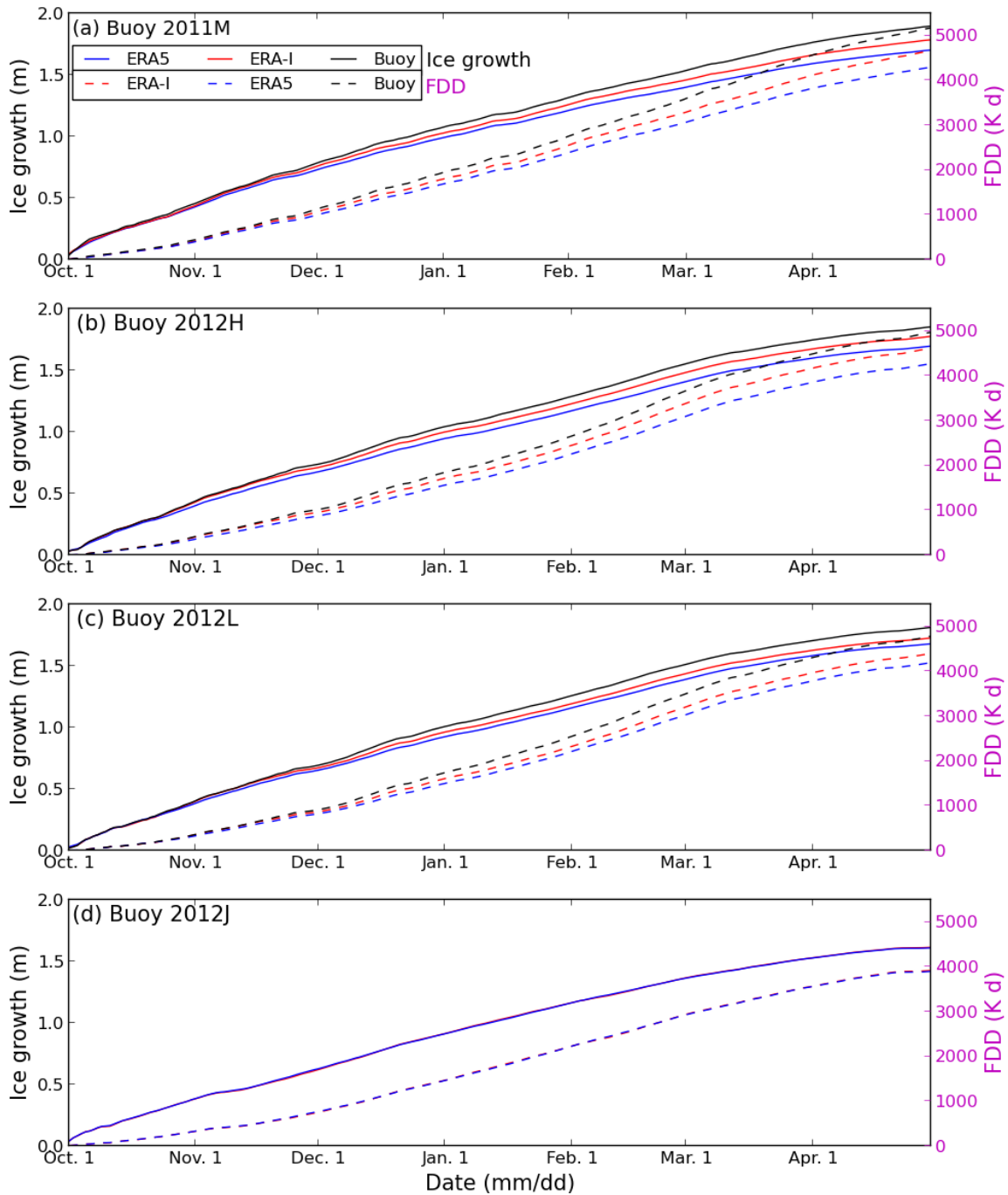
Fig. 7. FDD and estimated ice growth using cumulative FDD based on equation 1 along the trajectories of (a) Buoy 2011M, (b) Buoy 2012H, (c) Buoy 2012L, and (d) Buoy 2012J for freeze-up on 1 Oct.
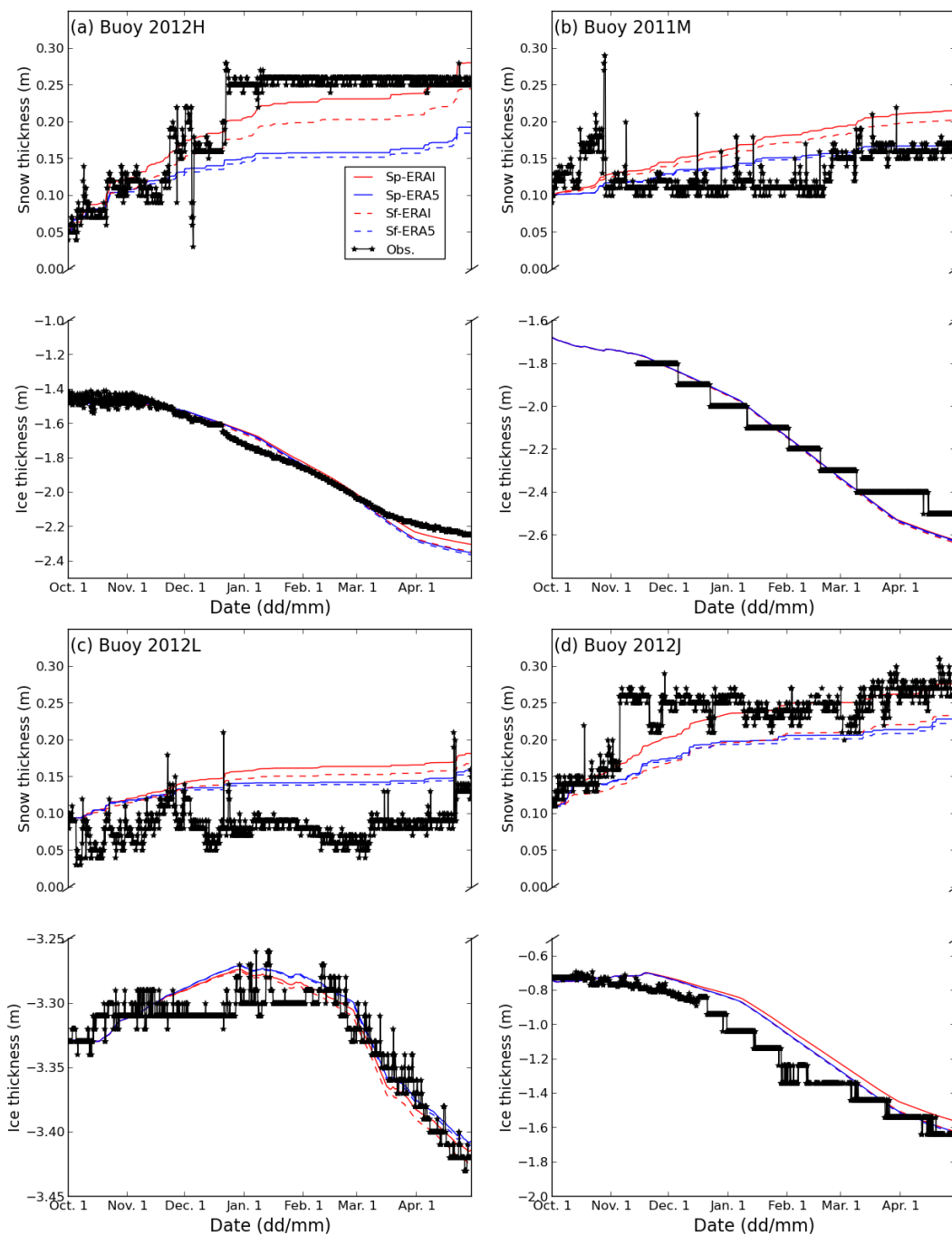
Fig. 8. Evolution of snow and sea ice during freezing season based on simulations with HIGHTSI for (a) Buoy 2012H, (b) Buoy 2011M, (c) Buoy 2012L, and (d) Buoy 2012J in the runs of Sp_ERAI, Sp_ERA5, Sf_ERAI, and Sf_ERA5.
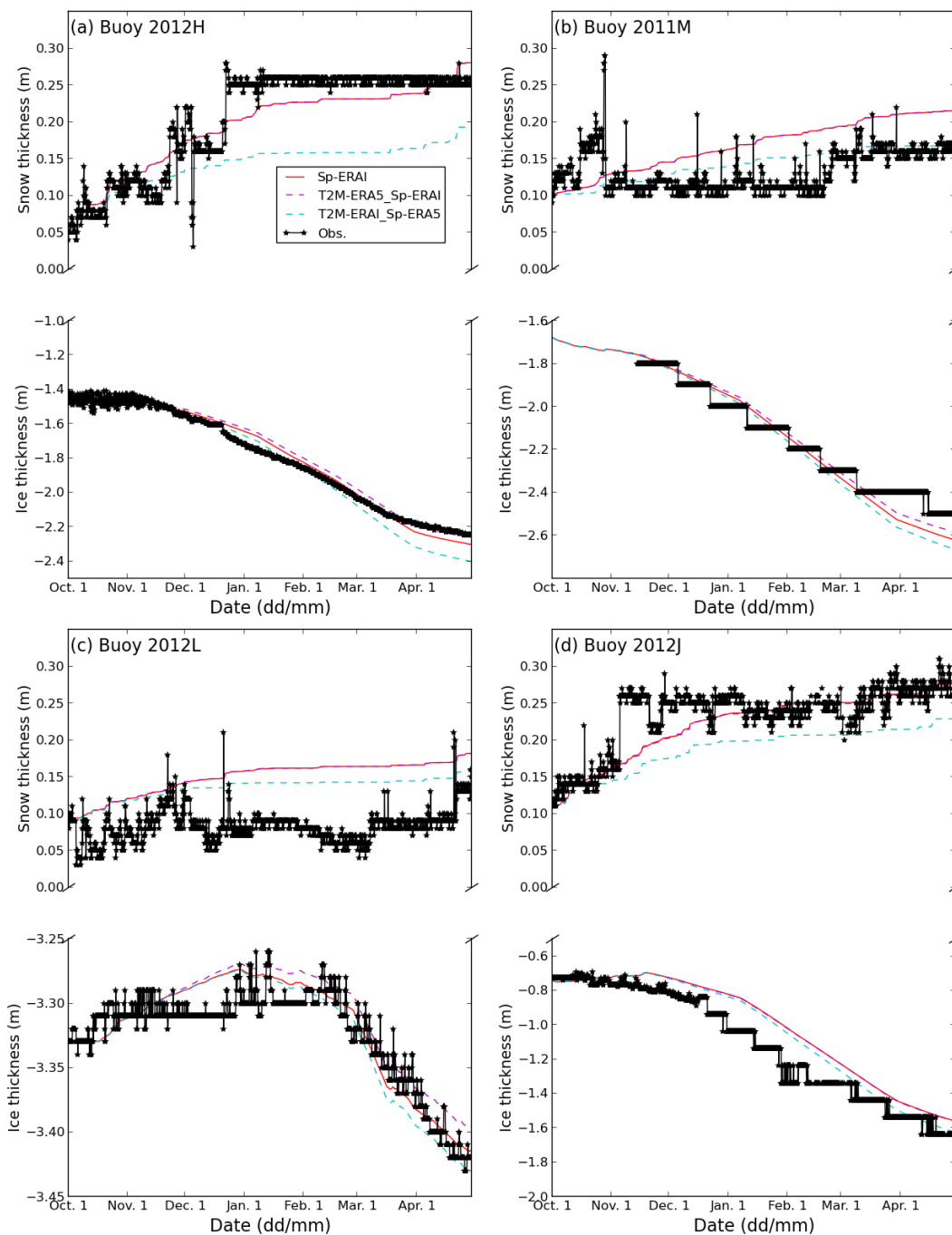
Fig. 9. Same as Fig. 8, but for the runs of T2M-ERA5, and T2M-ERAI_Sf-ERA5.